

Vapor–Liquid Equilibrium for Propionic Acid + *n*-Butyl Propionate from 60 to 101.3 kPa

Wen-Tzong Liu and Chung-Sung Tan*

Department of Chemical Engineering, National Tsing Hua University, Hsinchu, Taiwan 300, ROC

Isobaric vapor–liquid equilibrium data for propionic acid + *n*-butyl propionate mixtures at 60, 80, and 101.3 kPa were provided. From the measured data, it can be seen that the relative volatility was close to unity and no azeotrope occurred. The experimental data could be correlated by the NRTL, Wilson, and UNIQUAC thermodynamic models used to calculate activity coefficients of the liquid and the Hayden–O’Connell model for the association of propionic acid in the vapor. Double azeotropes at the pressures below 17.4 kPa were predicted by the NRTL and Hayden–O’Connell model. Both the negative and positive azeotrope temperatures were found to be close to those reported in the literature. The UNIFAC model with no adjustable parameters was also used in this study and was found to adequately describe the VLE behavior when the liquid-phase composition of propionic acid was below 0.85.

Introduction

n-Butyl propionate has been recognized as a green solvent for its low vapor pressure, good mixing capability, high electrical resistance, and acceptable odor.¹ The synthesis of *n*-butyl propionate is normally carried out by the esterification of propionic acid and *n*-butanol, but the separation of the resulting mixture is an energy-intensive process because of the relatively low volatility of the components and the existence of azeotropes.

Reactive distillation has been widely used in reversible reactions to eliminate the thermodynamic limitation and to result in a higher conversion. Esterification of carboxylic acids with alcohols is always limited by thermodynamic considerations due to its reversible nature and the presence of azeotropes. Its performance is believed to be enhanced using the reactive distillation technique. Prior to design of a reactive distillation process, knowledge of the thermodynamic behaviors of all the binaries and reaction kinetics is needed.

For the esterification of propionic acid and *n*-butanol, the vapor–liquid equilibria (VLE) data are available in the open literature for the four binary systems^{2–6} but not for the systems propionic acid + *n*-butyl propionate and water + *n*-butyl propionate. The VLE data for the system water + *n*-butyl propionate may be approximated by a set of NRTL parameters regressed from the liquid–liquid equilibrium data.⁷ With this approach, the predicted azeotrope was observed to be sufficiently close to the measured azeotrope.⁸ It is therefore rational to use the binary parameters obtained from this approach. For the system of propionic acid and *n*-butyl propionate, Kushner et al.⁹ observed the existence of an unusual biazeotrope at a pressure below 17.4 kPa, but the VLE data at the pressures near atmospheric pressure are not available in the literature.

In this study, the VLE data for the system of propionic acid and *n*-butyl propionate were measured with a dual-circulation operation. Several thermodynamic models were used to fit the experimental data. From the regression a thermodynamic model that is essential to the design of a reactive distillation process is provided.

Table 1. Physical and Chemical Properties of Propionic Acid and *n*-Butyl Propionate^a

	propionic acid	<i>n</i> -butyl propionate
chemical formula	C ₃ H ₆ O ₂	C ₇ H ₁₄ O ₂
molecular mass/kg·kmol ⁻¹	74.1	130.2
normal boiling point/K	414.3	418.6
radius of gyration/m	3.107 × 10 ⁻¹⁰	4.738 × 10 ⁻¹⁰
solubility parameter/(J·m ⁻³) ^{0.5}	1.946 × 10 ⁴	1.738 × 10 ⁴
van der Waals vol/m ³ ·kmol ⁻¹	0.0434	0.0835
van der Waals area/m ² ·kmol ⁻¹	6.530 × 10 ⁸	1.184 × 10 ⁹

^a The properties are extracted from DIPPR¹⁰ except the normal boiling point of *n*-butyl propionate.¹¹

Experimental Section

Propionic acid (Merck) and *n*-butyl propionate (TCI) with a purity of 99.8% were pretreated with 4A molecular sieves in order to remove the water present in these chemicals. The water content was analyzed with a Karl Fischer meter (Kyoto Electronics MKC-210) and was found to be less than 100 ppm after the treatment in both the chemicals. The physical and chemical properties of propionic acid and *n*-butyl propionate are given in Table 1.

The VLE measurements were carried out in a Fischer VLE apparatus (Fischer 0601). It consisted of an equilibrium cell of 100 cm³ equipped with a Pt-100 temperature sensor. The temperature in each phase could be maintained within ±0.1 K. To reach equilibrium rapidly at a given temperature and pressure, both vapor and liquid were circulated. The samples in the vapor and liquid phases taken by two solenoid valves located in the circulation loops were analyzed by a TCD gas chromatograph (Hewlett-Packard, 5980) with a column packed with 6% cyanopropylphenyl and 94% dimethyl polysiloxane.

In each measurement, a known amount of propionic acid and *n*-butyl propionate was charged into the equilibrium cell initially. When the pressure reached the desired value, the solution was heated to allow vaporization and condensation to occur in the equilibrium cell and in a condenser located above the cell, respectively. The measurements were carried out at the pressures 60, 80, and 101.3 kPa with an average deviation of ±0.03 kPa. A digital pressure

* Corresponding author. E-mail: cstan@che.nthu.edu.tw.

Table 2. VLE Data for the System Propionic Acid (1) and *n*-Butyl Propionate (2)

<i>T</i> /K	<i>x</i> ₁	<i>y</i> ₁	γ_1	γ_2	<i>T</i> /K	<i>x</i> ₁	<i>y</i> ₁	γ_1	γ_2
<i>P</i> = 60 kPa									
401.1	0.000	0.000	2.016	1.000	399.7	0.586	0.600	1.043	1.217
401.0	0.013	0.016	1.949	1.000	399.6	0.643	0.656	1.029	1.245
400.9	0.061	0.077	1.743	1.004	399.5	0.688	0.700	1.020	1.266
400.8	0.082	0.109	1.669	1.008	399.4	0.727	0.738	1.014	1.284
400.6	0.153	0.178	1.470	1.025	399.3	0.779	0.787	1.008	1.306
400.4	0.223	0.251	1.332	1.049	399.2	0.821	0.829	1.005	1.324
400.3	0.278	0.324	1.252	1.070	399.1	0.871	0.878	1.002	1.343
400.0	0.383	0.407	1.146	1.118	398.8	0.935	0.940	1.001	1.365
399.9	0.435	0.438	1.114	1.142	398.4	1.000	1.000	1.000	1.385
399.8	0.512	0.536	1.070	1.181					
<i>P</i> = 80 kPa									
410.2	0.046	0.058	1.785	1.003	408.4	0.616	0.637	1.036	1.230
410.1	0.077	0.098	1.673	1.007	408.2	0.692	0.703	1.020	1.266
409.8	0.162	0.174	1.444	1.027	408.0	0.747	0.761	1.012	1.291
409.5	0.229	0.262	1.320	1.050	407.9	0.798	0.807	1.007	1.313
409.1	0.316	0.332	1.207	1.085	407.8	0.833	0.850	1.004	1.328
409.0	0.372	0.390	1.155	1.111	407.7	0.901	0.915	1.001	1.354
408.8	0.441	0.462	1.107	1.144	407.3	0.955	0.967	1.000	1.373
408.7	0.472	0.492	1.089	1.159	407.0	1.000	1.000	1.000	1.387
<i>P</i> = 101.3 kPa									
418.2	0.062	0.083	1.712	1.004	415.9	0.643	0.663	1.030	1.241
418.0	0.089	0.105	1.625	1.009	415.7	0.700	0.715	1.019	1.268
417.8	0.131	0.155	1.510	1.018	415.5	0.750	0.767	1.012	1.291
417.5	0.193	0.221	1.379	1.036	415.3	0.807	0.822	1.006	1.316
417.2	0.267	0.297	1.264	1.063	415.0	0.860	0.871	1.003	1.338
416.9	0.362	0.392	1.164	1.104	414.6	0.929	0.937	1.001	1.364
416.6	0.452	0.479	1.101	1.147	414.3	1.000	1.000	1.000	1.388
416.3	0.530	0.549	1.064	1.185					

indicator with an accuracy of 0.01 kPa was used to monitor the pressure in each measurement. The equilibrium was considered to be reached when the temperature difference between the liquid and vapor phases was within ± 0.1 K and the variation in mole fraction was less than 0.0005.

Results and Discussion

The measured compositions of propionic acid in the vapor and liquid phases are shown in Table 2. The thermodynamic consistency was tested using the Herington method with a tolerance of 10%. It was found that the data could be thermodynamically consistent when the association of propionic acid in the vapor phase was considered; but it was not the case when the ideal gas assumption was applied. The reproducibility tests on both the compositions in the vapor and liquid phases were performed at all the operating temperatures and pressures. The deviation in composition was observed to be less than 3.0%.

Because carboxylic acids are always present in an associated form, like a dimer or trimer, in both the vapor and liquid phases even at low pressures,^{12–14} a significant deviation in fugacity coefficient may exist using the ideal gas assumption.^{15–18} To account for the nonideal behavior, a chemical theory is commonly used to calculate the fugacity coefficient in vapor. In this study, the Hayden–O'Connell (HOC) model was used for this purpose.¹⁹ The Poynting correction factor was also included in the calculation of fugacity at the reference state. The liquid molar volumes were evaluated from the modified Rackett equation.²⁰ The vapor pressures of propionic acid (1) and *n*-butyl propionate (2) were evaluated from the following extended Antoine equations,¹⁰

$$\ln(P_1^{\text{sat}}) = 57.16 - 7279/T - 4.652 \ln T + (4.851 \times 10^{-19})T^6 \quad (1)$$

$$\ln(P_2^{\text{sat}}) = 85.27 - 8183/T - 9.091 \ln T + (3.911 \times 10^{-6})T^2 \quad (2)$$

where P^{sat} is in pascal and T is in kelvin.

To account for the effect of the nonideal behavior of a liquid solution containing hydrogen bonding on the activity coefficient, the excess free energy models are widely used.²¹ In this study, three models of this kind (NRTL, Wilson, and UNIQUAC) were employed. The equations for these three models are written as follows.

For the NRTL model,²²

$$\ln \gamma_1 = x_2^2 \left[\tau_{21} \left(\frac{G_{21}}{x_1 + x_2 G_{21}} \right)^2 + \frac{\tau_{12} G_{12}}{(x_2 + x_1 G_{12})^2} \right] \quad (3)$$

$$\ln \gamma_2 = x_1^2 \left[\tau_{12} \left(\frac{G_{12}}{x_2 + x_1 G_{12}} \right)^2 + \frac{\tau_{21} G_{21}}{(x_1 + x_2 G_{21})^2} \right] \quad (4)$$

where

$$\tau_{12} = \frac{A_{12}}{RT}, \quad \tau_{21} = \frac{A_{21}}{RT}$$

$$G_{12} = \exp(-\alpha\tau_{12}); \quad G_{21} = \exp(-\alpha\tau_{21})$$

Walas²¹ suggested to use $\alpha = 0.3$ for nonaqueous mixtures. This value was thus chosen in the present regression.

For the Wilson model,²³

$$\ln \gamma_1 = -\ln(x_1 + x_2 \Lambda_{12}) + x_2 \left(\frac{\Lambda_{12}}{x_1 + x_2 \Lambda_{12}} - \frac{\Lambda_{21}}{x_2 + x_1 \Lambda_{21}} \right) \quad (5)$$

$$\ln \gamma_2 = -\ln(x_2 + x_1 \Lambda_{21}) - x_1 \left(\frac{\Lambda_{12}}{x_1 + x_2 \Lambda_{12}} - \frac{\Lambda_{21}}{x_2 + x_1 \Lambda_{21}} \right) \quad (6)$$

$$\Lambda_{12} = \frac{V_2^{\text{L}}}{V_1^{\text{L}}} \exp\left(\frac{-A_{12}}{RT}\right) \quad (7)$$

$$\Lambda_{21} = \frac{V_1^{\text{L}}}{V_2^{\text{L}}} \exp\left(\frac{-A_{21}}{RT}\right) \quad (8)$$

where V^{L} is the molar volume of liquid component i .

For the UNIQUAC model,²⁴

$$\ln \gamma_i = \ln \gamma_i(\text{combinatorial}) + \ln \gamma_i(\text{residual})$$

$$\ln \gamma_1(\text{combinatorial}) =$$

$$\ln \frac{\phi_1}{x_1} + \frac{z}{2} q_1 \ln \frac{\theta_1}{\phi_1} + \phi_2 \left(l_1 - \frac{r_1}{r_2} l_2 \right) \quad (9)$$

$$\ln \gamma_1(\text{residual}) =$$

$$-q_1 \ln(\theta_1 + \theta_2 \tau_{21}) + \theta_2 q_1 \left(\frac{\tau_{21}}{\theta_1 + \theta_2 \tau_{21}} - \frac{\tau_{12}}{\theta_1 \tau_{12} + \theta_2} \right) \quad (10)$$

$$\ln \gamma_2(\text{combinatorial}) =$$

$$\ln \frac{\phi_2}{x_2} + \frac{z}{2} q_2 \ln \frac{\theta_2}{\phi_2} + \phi_1 \left(l_2 - \frac{r_2}{r_1} l_1 \right) \quad (11)$$

$$\ln \gamma_2(\text{residual}) =$$

$$-q_2 \ln(\theta_2 + \theta_1 \tau_{12}) + \theta_1 q_2 \left(\frac{\tau_{12}}{\theta_1 \tau_{12} + \theta_2} - \frac{\tau_{21}}{\theta_1 + \theta_2 \tau_{21}} \right) \quad (12)$$

Table 3. Adjustable Binary Parameters Obtained from the Regression for the System Propionic Acid (1) and *n*-Butyl Propionate (2)

thermodynamic model	$A_{12}/\text{J}\cdot\text{mol}^{-1}$	$A_{21}/\text{J}\cdot\text{mol}^{-1}$	α	AARD
NRTL-HOC	-2007.65	4741.87	0.3	0.0324
Wilson-HOC	-3748.66	1106.85		0.0326
UNIQUAC-HOC	1754.73	-3335.18		0.0366

where

$$l_i = (r_i - q_i)z/2 - (r_i - 1), \quad z = 10$$

$$\theta_i = \frac{q_i x_i}{\sum_j q_j x_j} \text{ is the area fraction of component } i$$

$$\phi_i = \frac{r_i x_i}{\sum_j r_j x_j} \text{ is the volume fraction of component } i$$

$$\tau_{12} = \exp\left(\frac{-A_{12}}{RT}\right)$$

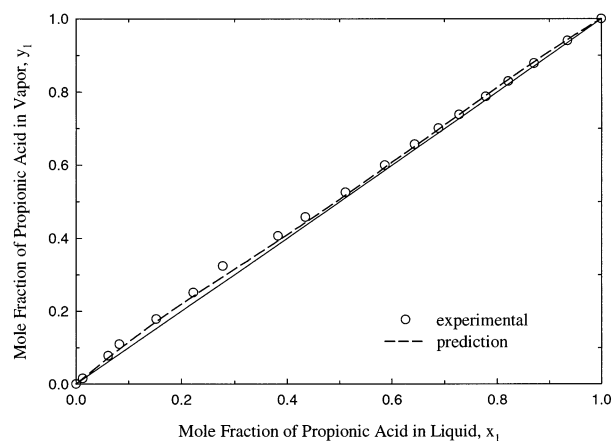
$$\tau_{21} = \exp\left(\frac{-A_{21}}{RT}\right)$$

In the above three models, A_{12} and A_{21} are the binary interactive parameters to be determined by regression. The regression was carried out using the Aspen Plus chemical process simulator,²⁵ in which the generalized least-squares method, the maximum-likelihood principle, and the Britt-Luecke algorithm were used to minimize the average absolute relative deviation (AARD), defined as

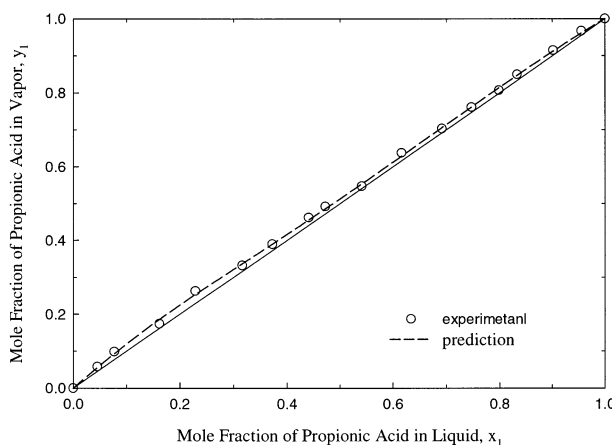
$$\text{AARD} = \sum_i^n |(T_i - T_m)/T_m|/n + \sum_i^n |(x_i - x_m)/x_m|/n + \sum_i^n |(y_i - y_m)/y_m|/n \quad (13)$$

The binary interaction parameters evaluated from the regression for these three models are shown in Table 3. It can be seen that the NRTL model provided the best fit, though the other two models could also fit the experimental data well. Under this circumstance, the NRTL-HOC model was chosen to investigate the vapor-liquid behavior for the system propionic acid + *n*-butyl propionate. No azeotrope was predicted by this model, as shown in Figure 1. Figure 2 shows that the calculated activity coefficients of propionic acid and *n*-butyl propionate exhibited a positive deviation from the ideality and a sharp increase in activity coefficient of propionic acid in the dilute region. This observation followed the general trend for an associated carboxylic acid dissolved in a nonassociated component.²⁶ Figure 3 illustrates the temperature dependence of the activity coefficient of propionic acid. In a dilute region, the activity coefficient of propionic acid decreases with increasing temperature. This was due to a decrease in the equilibrium constant for association as temperature increased, since association was exothermic.²⁶ From the calculated activity coefficients, the Gibbs excess free energy could then be evaluated using the equation

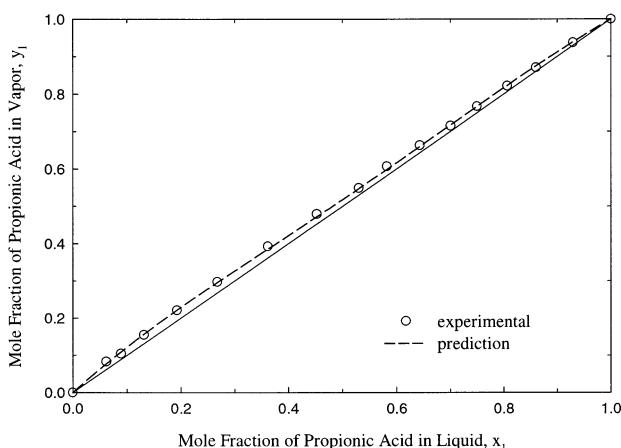
$$G^E = RT(x_1 \ln \gamma_1 + x_2 \ln \gamma_2) \quad (14)$$



(a)



(b)



(c)

Figure 1. x - y diagram for the system propionic acid (1) and *n*-butyl propionate (2) at (a) 60 kPa, (b) 80 kPa, and (c) 101.3 kPa.

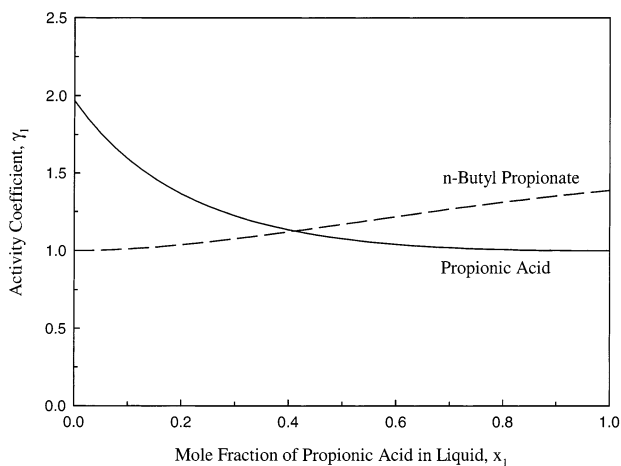
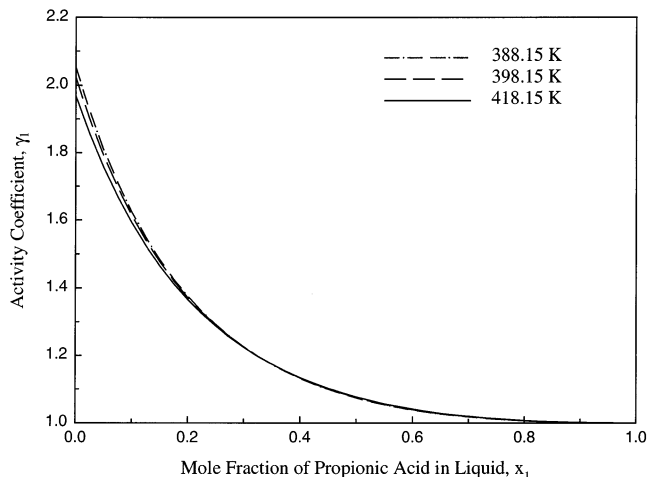
From the calculated G^E at 101.3 kPa shown in Figure 4, it is seen that the maximum of the calculated G^E did not appear at $x = 0.5$ (regular solution) and a higher temperature resulted in a higher G^E .

Kushner et al.⁹ observed a double azeotrope at pressures below 17.4 kPa for the present system. A polyazeotrope in binary systems is not common and is reported in the following systems: water + dinitrogen oxide,²⁷ benzene + hexafluorobenzene,²⁸ methanol + diethylamine,²⁹ 1,2-butylene oxide + methyl acetate,³⁰ and acetic acid + isobutyl acetate.³¹ The polyazeotrope is mainly attributed to the association effects in both the liquid and vapor phases.¹⁷

Table 4. Comparison of Double Azeotropes between the Predicted and the Experimental Data

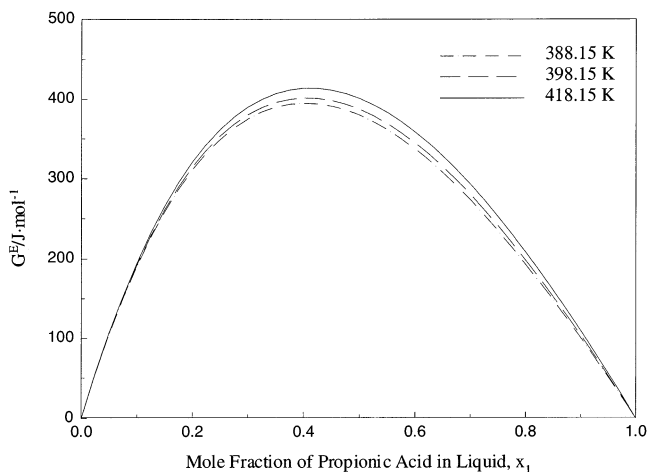
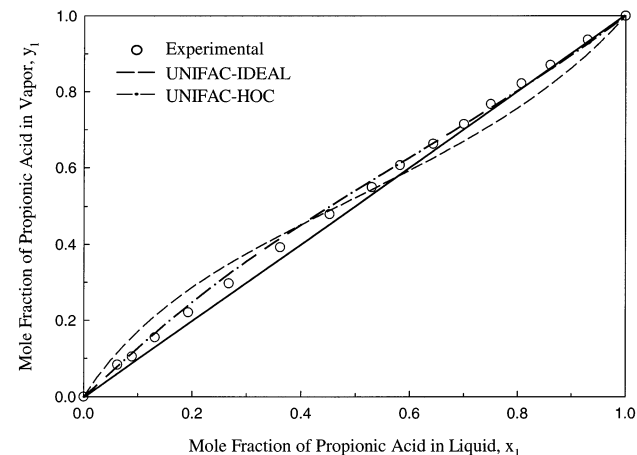
P/kPa	boiling point 1/K		PA ^c /mol %		boiling point 2/K		PA ^c /mol %	
	ref 9 ^a	model ^b	ref 9 ^a	model ^b	ref 9 ^a	model ^b	ref 9 ^a	model ^b
17.4	365.8	365.5	20	14.5	92.9	92.7	77.5	49.8
14.0	361.2	360.2	15.5	12.4	87.8	88.4	80.1	69.5
9.7		351.6	7.4		79.5	79.7	82.5	86.4
7.0	344.8			5.4	72.3		85.1	
6.7					71.5	71.8	85.0	93.6
4.4	334.6			1.9	62.9	63.2	87.4	97.3
3.8	331.5			1.0	59.8		87.5	
3.2					56.5	57.1	87.5	98.0
2.4					51.3	51.4	90.0	98.8

^a Experimental data from Kushner et al.⁹ ^b Model predicted in this study. ^c PA denotes propionic acid composition.

**Figure 2.** Activity coefficients of propionic acid (1) and *n*-butyl propionate (2) as a function of composition at 498.15 K.**Figure 3.** Activity coefficients of propionic acid (1) as a function of composition at different temperatures.

While no azeotrope was observed experimentally in the presently studied pressure range from 60 to 101.3 kPa, a double azeotrope is predicted at the pressures below 17.4 kPa using the NRTL–HOC model with the binary parameters provided in Table 3. Both the negative azeotrope and positive azeotrope are very close to those reported by Kushner et al.,⁹ but the compositions of the azeotropes were of a substantial deviation, as shown in Table 4.

The UNIFAC model³² with no adjustable parameter was also employed to test its applicability in this study. The predicted VLE shown in Figure 5 reveals that the model considering the vapor-phase nonideality (UNIFAC–HOC) was adequate to describe the VLE behavior when the liquid molar composition of propionic acid was less than 0.85. But

**Figure 4.** Excess Gibbs energies as a function of x_1 at different temperatures.**Figure 5.** Comparison of the UNIFAC models with the experimental data at 101.3 kPa.

it failed to describe VLE at the higher propionic acid compositions because an azeotrope, not observed experimentally, was predicted in this model. When the UNIFAC model accompanying the ideal gas assumption (UNIFAC–IDEAL) was employed, a substantial deviation was observed, as shown in Figure 5.

Conclusions

Vapor–liquid equilibrium data for the system propionic acid and *n*-butyl propionate were measured at 60, 80, and 101.3 kPa by using a dual circulation technique. The experimental data were fitted with the NRTL, Wilson, and UNIQUAC models that were used to calculate activity coefficients in the liquid phase and the Hayden–O’Connell

model that was used to account for the association of propionic acid in the vapor phase. The regression showed that all these models could correlate the experimental data satisfactorily. With the fitted binary parameters in the NRTL and Hayden–O'Connell model, a double azeotrope was predicted to occur at a pressure below 17.4 kPa. Both the negative and positive azeotrope temperatures were found to be sufficiently close to those reported by Kushner et al.⁹ In addition to these models, the UNIFAC model with no adjustable parameter was found to be adequate to predict the VLE behavior when the liquid-phase composition of propionic acid was below 0.85.

Nomenclature

A_{ij} = binary parameters

G^E = excess Gibbs energy/cal·mol⁻¹

G_{ij} = parameter in the NRTL model

n = total number of data points

R = gas constant

r_i = parameter in the UNIQUAC model

q_i = parameter in the UNIQUAC model

T = temperature calculated in regression (K)

T_m = temperature measured in experiment (K)

x_i = liquid composition calculated in regression

x_{m_i} = liquid composition measured in experiment

y_i = vapor composition calculated in regression

y_{m_i} = vapor composition measured in experiment

z = parameter in the UNIQUAC model

Greek Letters

α = binary parameter in the NRTL model

γ_i = activity coefficient of species i

$\gamma_i(\text{combinatorial})$ = activity coefficient accounting for the combinatorial part of species i

$\gamma_i(\text{residual})$ = activity coefficient accounting for the residual part of species i

θ_i = parameter in the UNIQUAC model

ϕ_i = parameter in the UNIQUAC model

τ_{ij} = parameter in the UNIQUAC model

Literature Cited

- (1) Sullivan, D. A. Solvent selection in today's regulatory environment. *Mod. Paint Coat.* **1995**, Nov, 38–42.
- (2) Amer Amezaga, S. *An. Quim.* **1975**, 71, 127.
- (3) Amer Amezaga, S. *An. Quim.* **1975**, 71, 117–126.
- (4) Ellis, S. R. M.; Garbett, R. D. *Ind. Eng. Chem.* **1960**, 52, 385.
- (5) Hessel, D. *Phys. Chem.* **1965**, 229, 199.
- (6) Gonzalez, E.; Ortega, J. Densities and isobaric vapor-liquid equilibria for the mixtures formed by four butyl esters and 1-butanol. *J. Chem. Eng. Data* **1996**, 41, 53–58.
- (7) Bridgman, J. A. *Ind. Eng. Chem.* **1928**, 20, 184.
- (8) Horseley, L. H. Azeotropic Data-III. *Advances in Chemistry Series 116*; American Chemical Society: Washington, DC, 1973.
- (9) Kushner, T. M.; Shutova, G. V.; Raeva, V. M.; Serafimov, L. A. Biazotropy in the propionic acid-butyl propionate system. *Russ. J. Phys. Chem.* **1992**, 66, 445–447.
- (10) DIPPR, *Data Compilation of Pure Compound Properties*; Standard Reference Data; National Institute of Science and Technology: Gaithersburg, MD, 1985.

- (11) Weast, R. C.; Grasselli, J. G. *CRC Handbook of Data on Organic Compounds*, 2nd ed.; CRC Press: Boca Raton, FL, 1989.
- (12) Sawistowski, H.; Pllavakls, A. Vapor-liquid equilibrium with association in both phases. Multicomponent system containing acetic acid. *J. Chem. Eng. Data* **1982**, 27, 64–71.
- (13) Sebastiani, E.; Lacquaniti, L. Acetic acid–water system thermodynamical correlation of vapor-liquid equilibrium data. *Chem. Eng. Sci.* **1967**, 22, 1155–1162.
- (14) Tsonopoulos, C.; Prausnitz, J. M. Fugacity coefficients in vapor-phase mixtures of water and carboxylic acids. *Chem. Eng. J.* **1970**, 1, 273–278.
- (15) Rhim, J. K.; Bae, S. Y.; Lee, H. T. Isothermal vapor-liquid equilibrium accompanied by esterification. ethanol-formic acid system. *Int. Chem. Eng.* **1985**, 25 (3), 551–557.
- (16) Kang, Y. W.; Lee, Y. Y.; Lee, W. K. Vapor-liquid equilibria with chemical reaction equilibrium- Systems containing acetic acid, ethyl alcohol, water, and ethyl acetate. *J. Chem. Eng. Jpn.* **1982**, 25 (6), 649–655.
- (17) Segura, H.; Wisniak, J.; Aucejo, A.; Monton, J. B.; Munoz, R. Polyazetropy in binary systems. 2. Association effects. *Ind. Eng. Chem. Res.* **1996**, 35, 4194–4202.
- (18) Tamir, A.; Wisniak, J. Vapor equilibrium in associating systems (water-formic acid-propionic acid). *Ind. Eng. Chem. Fundam.* **1976**, 15, 274–280.
- (19) Hayden, J. G.; O'Connell, J. P. A generalized method for predicting second virial coefficients. *Ind. Eng. Chem. Process Des. Dev.* **1975**, 14 (3), 209–216.
- (20) Reid, R. C.; Prausnitz, J. M.; Poling, B. E. *The Properties of Gases & Liquids*, 4th ed.; McGraw-Hill: New York, 1988.
- (21) Walas, S. M. *Phase Equilibria in Chemical Engineering*; Butterworth: Boston, 1985.
- (22) Renon, H.; Prausnitz, J. M. Local compositions in thermodynamic excess functions for liquid mixtures. *AIChE J.* **1968**, 14, 135–144.
- (23) Wilson, G. M. Vapor-liquid equilibrium. XI: A new expression for the excess free energy of mixing. *J. Am. Chem. Soc.* **1964**, 86, 127–130.
- (24) Abrams, D. S.; Prausnitz, J. M. Statistical thermodynamics of liquid mixtures: A new expression for the excess Gibbs energy of partly or completely miscible systems. *AIChE J.* **1975**, 21, 116–128.
- (25) *ASPEN PLUS, User Guide*, Release 10; Aspen Technology Inc.: Cambridge, MA, 1998.
- (26) Prausnitz, J. M.; Lichtenthaler, R. N.; de Azevedo, E. G. *Molecular Thermodynamics of Fluid-Phase Equilibria*, 3rd ed.; Prentice Hall: Upper Saddle River, NJ, 1999.
- (27) Lloyd, L.; Wyatt, P. A. H. The vapour pressures of nitric acid solutions. Part I. New azeotropes in the water-dinitrogen pentoxide system. *J. Chem. Soc.* **1955**, 2249–2252.
- (28) Gaw, W. J.; Swinton, F. L. Thermodynamic properties of binary systems containing hexafluorobenzene. Part 4.-Excess Gibbs free energies of the three systems hexafluorobenzene + benzene, toluene, and *p*-xylene. *Trans. Faraday Soc.* **1968**, 64, 2023–2034.
- (29) Sristava, R.; Smith, B. D. Total pressure vapor liquid equilibrium data for binary systems of diethylamine with acetone, acetonitrile and methanol. *J. Chem. Eng. Data* **1985**, 30, 308–313.
- (30) Leu, A. D.; Robinson, D. B. Vapor-Liquid Equilibrium in Selected Binary Systems of Interest to the Chemical Industry. In *Experimental Results for Phase Equilibria and Pure Component Properties*; DIPPR Data Series 1; Cunningham, J. R., Johns, D. K., Eds.; DIPPR: New York, 1991.
- (31) Christensen, S.; Olson, J. Phase equilibria and multi azeotrope of the acetic acid-isobutyl acetate. *Fluid Phase Equilib.* **1992**, 79, 187–199.
- (32) Fredenslund, A.; Jones, R. L.; Prausnitz, J. M. Group-contribution estimation of activity coefficients in nonideal liquid mixtures. *AIChE J.* **1975**, 21, 1086–1098.

Received for review February 15, 2002. Accepted September 24, 2002.

JE0255168